Kidney International, Vol. 62 (2002), pp. 1672–1681

Expression profiling confirms the role of endocytic receptor megalin in renal vitamin D_3 metabolism

JAN HILPERT, LISE WOGENSEN, THOMAS THYKJAER, MAREN WELLNER, UWE SCHLICHTING, TORBEN F. ORNTOFT, SEBASTIAN BACHMANN, ANDERS NYKJAER, and THOMAS E. WILLNOW

Max-Delbrueck-Center for Molecular Medicine and Medical Faculty of the Free University of Berlin, Institute for Anatomy and Franz-Volhard-Clinic, Humboldt University of Berlin, Berlin, and Department of Nephrology, Medical School Hannover, Hannover, Germany; Research Laboratory for Biochemical Pathology, Aarhus University Hospital, and AROS Applied Biotechnology ApS, Department of Clinical Biochemistry, Skejby University Hospital, and Department of Medical Biochemistry, University of Aarhus, Aarhus, Denmark

Expression profiling confirms role of endocytic receptor megalin in renal vitamin D_3 metabolism.

Background. The endocytic receptor megalin constitutes the major pathway for clearance of low-molecular weight plasma proteins from the glomerular filtrate into the renal proximal tubules. Furthermore, the receptor has been implicated in a number of other functions in the kidney including uptake and activation of 25-(OH) vitamin D_3, calcium and sodium reabsorption as well as signal transduction.

Methods. We used genome-wide expression profiling by microarray technology to detect changes in the gene expression pattern in megalin knockout mouse kidneys and to uncover some of the renal pathways affected by megalin deficiency.

Results. Alterations were identified in several (patho)physiologic processes in megalin-deficient kidneys including the renal vitamin D metabolism, transforming growth factor (TGF)-β1 signal transduction, lipid transport and heavy metal detoxification. Most importantly, changes were detected in the mRNA levels of 25-(OH) vitamin D-24-hydroxylase and 25-(OH) vitamin D-1α-hydroxylase as well as strong up-regulation of TGF-β1 target genes. Both findings indicate plasma vitamin D deficiency and lack of vitamin D signaling in renal tissues.

Conclusions: Expression profiling confirms a crucial role for megalin in renal vitamin D metabolism.

Megalin is a member of the low-density lipoprotein receptor gene family highly expressed on the luminal surface of the proximal tubular epithelium [1–6]. It constitutes the major endocytic pathway in proximal tubules for the clearance of filtered low-molecular weight plasma proteins [7–9]. Consistent with a crucial role of megalin in tubular uptake processes, megalin-deficient mice suffer from tubular resorption deficiency and low-molecular weight proteinuria [9].

Recent work suggests important new functions for megalin that extend beyond mere clearance of proteins from the glomerular filtrate. Megalin was shown to mediate the tubular uptake of complexes of 25-(OH) vitamin D_3 with its plasma carrier, the vitamin D-binding protein (DBP) [10]. In megalin-deficient mice, lack of the receptor results in an inability to retrieve 25-(OH) vitamin D_3/DBP complexes from the glomerular filtrate and in urinary excretion of the vitamin [9, 10]. This finding indicated an essential role of the receptor in renal vitamin D_3 homeostasis. Other studies have demonstrated that megalin interacts with several membrane proteins expressed in proximal tubular cells. These proteins include cubilin, a peripheral membrane protein responsible for tubular retrieval of albumin [11, 12], and the apical Na^+/H^+ exchanger isoform 3 (NHE3) [13]. Association of cubilin with megalin is required for recycling of cubilin through the endocytic compartments of the cells [11, 14]. The significance of megalin for NHE3 activity and tubular sodium reabsorption is unclear at present. Finally, megalin has been shown to harbor binding sites for cytosolic adaptor proteins in its cytoplasmic domain [15–18]. Because these adaptors also interact with components of the cellular signal transduction machinery (such as, non-receptor tyrosine kinases), megalin is suspected to directly participate in signaling in the kidney.

Megalin knockout mice represent a unique model to test the contribution of the receptor to various physiological processes. Unfortunately, megalin$^{-/-}$ mice suffer from a developmental defect of the forebrain causing perinatal lethality of most affected animals [19]. Only approximately 1 to 2% of the megalin$^{-/-}$ animals survive the perinatal period and grow up to adulthood [9, 10]. The small number of survivors so far precluded an in-depth

Key words: 25-(OH) vitamin D-1α-hydroxylase, microarray analysis, renal proximal tubules, transforming growth factor-β1, low density lipoprotein.

Received for publication April 8, 2002
and in revised form May 30, 2002
Accepted for publication June 21, 2002

investigation of the (patho)physiologic consequences of the receptor gene defect in vivo. However, recent technological advances in genome-wide expression profiling by microarrays now enable us to uncover pathologic processes in tissues based on changes in the gene expression pattern even in smaller number of samples [20]. Using the oligonucleotide microarray technology we investigated the alterations in the gene expression profile in kidneys from megalin-deficient as compared to wild type mice. We detected changes in the gene expression pattern that confirm a role of the receptor in renal vitamin D metabolism.

METHODS

Animals

The generation of megalin-deficient mice has been described before [19]. The animals were bred in-house and fed ad libitum a normal mouse chow diet containing 1% calcium, 0.7% phosphorus and 1.000 IU vitamin D_3 (V1126 Extrudat diet; Sniff, Sost, Germany). Littermates of heterozygous breeding were used for comparative expression profiling at the age of 12 to 16 weeks. A total of four experiments were performed comparing two male and two female megalin-deficient animals and their matched controls.

cRNA preparation

Total RNA was prepared from kidney tissues applying the Trizol® method (Gibco-BRL; *www.lifetech.com*). The first and second strand cDNA synthesis was performed using the SuperScript Choice System (Life Technologies, *www.invitrogen.com*), labeled cRNA was prepared using the BioArray High Yield RNA Transcript Labeling Kit (Enzo, *www.enzobio.com*). Biotin-labeled cytidine 5′-triphosphate (CTP) and uridine triphosphate (UTP; Enzo) were used in this reaction together with unlabeled nucleotide triphosphates (NTPs). Non-incorporated nucleotides were removed using RNeasy columns (Qiagen, *www.qiagen.com*).

Array hybridization and scanning

Fifteen micrograms of cRNA were fragmented at 94°C for 35 minutes in buffer containing 40 mmol/L Tris-acetate pH 8.1, 100 mmol/L KOAc, 30 mmol/L MgOAc. Prior to hybridization, the fragmented cRNA was heated to 95°C for five minutes in a 6× SSPE-T hybridization buffer (1 mol/L NaCl, 10 mmol/L Tris, pH 7.6, 0.005% Triton) and subsequently to 40°C for five minutes before loading onto the Affymetrix probe array cartridge. The probe array (Mu11K chip B; Affymetrix, *www.affymetrix.com*) was incubated for 16 hours at 45°C, consecutive washing and staining steps were performed in the Affymetrix Fluidics Station. The biotinylated cRNA was stained with a streptavidin-phycoerythrin conjugate (Molecular Probes, *www.probes.com*) at a final concentration of 2 μg/μL in 6× SSPE-T for 30 minutes at 25°C, followed by 10 washes in 6× SSPE-T at 25°C. An antibody amplification step was added using 0.1 mg/mL goat IgG (Sigma, *www.sigma.com*) and 3 μg/mL biotinylated goat anti-streptavidin antibody (Vector Laboratories, *www.vectorlabs.com*). These incubations were followed by a staining step with a streptavidin-phycoerythrin conjugate at a final concentration of 2 μg/μL in 6× SSPE-T for 30 minutes at 25°C, followed by 10 washes in 6× SSPE-T at 25°C. The probe arrays were scanned at 560 nm using a confocal laser-scanning microscope. The readings from the quantitative scanning were analyzed by the Affymetrix Gene Expression Analysis Software. For array-to-array comparison, the readings were scaled to a global intensity of 150, as previously published [21].

Quantitative RT-PCR

Quantitative reverse transcription-polymerase chain reaction (RT-PCR) was performed on total RNA samples from wild type and megalin-deficient littermates using Taq-man® technology (Applied Biosystems, *www.appliedbiosystems.com*). The following oligonucleotides were used for 25-(OH) vitamin D-1α-hydroxylase: forward 5′-TCAGATGTTTGCCTTTGCCC-3′, reverse 5′-TGG TCCTCATCGCAGCTTC-3′ and the probe Fam 5′-AGG CACGTGGAGCTGCGAGAAGG-3′ Tamra; for 25-OH-vitamin D-24-hydroxylase: forward 5′-GAGCCTGC TGGAAGCTCTGT-3′, reverse 5′-GGTTTGATCTCT AGCCGCTGG-3′ and the probe Fam 5′-CCGCACAG AGAGCGCGCATC-3′ Tamra; for C/EBP: forward 5′-AAGAGCCGCGACAAGGC-3′, reverse 5′-GTCAGC TCCAGCACCTTGTG-3′, and the probe Fam 5′-AAG ATGCGCAACCTGGAGACGCA-3′ Tamra; and for collagen IIIα-1: forward 5′-GATGTCGTTGATGTGA GCTG-3′, reverse 5′-GCAGTGGTATGTAATGTCT CTGGGA-3′ and the probe Fam 5′-ATTCCTCAGAC TTCTTTCCAGCCGGG-3′ Tamra.

Determination of endocrine and TGF-β1 parameters

For urine collection, mice were placed in metabolic cages for 16 hours and given 10% sucrose in the drinking water to increase urine excretion. Urine samples obtained were qualitatively indistinguishable from samples collected without sucrose load as shown by total output of ions, amino acids, creatinine, and by pH (not shown). PTH 1-38 fragments in urine and plasma were measured by a radioimmunoassay, vitamin D_3 metabolites by standard competitive protein binding assay (Immundiagnostik). TGF-β1 levels in plasma and in kidney homogenates were determined using the TGF-β1 E_{max} Immunoassay Systems (Promega, *www.promega.com*). Prior to analysis, latent TGF-β1 was activated to the immunoreactive form by incubation of the samples in 0.1 N HCl for 15

minutes at room temperature, followed by neutralization with 1 N NaOH.

In situ hybridization

Deparaffinized sections were deproteinated in proteinase K solution (10 μg/mL) for 30 minutes at 20°C and prehybridized for three hours at 45°C in a buffer composed of 50% formamide, 0.3 mol/L NaCl, 20 mmol/L Tris pH 8.0, 5 mmol/L ethylenediaminetetraacetic acid (EDTA), 1 × Denhart's solution, 10% dextran sulfate and 10 mmol/L dithiothreitol (DTT). Hybridization with ^{35}S-UTP-labeled sense or antisense RNA probes (6×10^5 cpm/section) was carried out for 16 hours at 50°C, followed by washing, dehydration and exposure. RNA probes were prepared by in vitro transcription of a plasmid containing the collagen type IIIα1 cDNA (H. Eberspaecher, UT Anderson Cancer Center, Houston, TX, USA).

Immunohistology

Kidneys were fixed in situ by consecutive infusions with 70 mmol/L sucrose, followed by 3% paraformaldehyde in phosphate-buffered saline (PBS), and 150 mmol/L sucrose. Cryosections (5 μm) were incubated with rabbit anti-rat collagen IIIα1 antibody (BioLogo; 1:200 dilution) for one hour at room temperature, followed by peroxidase-conjugated anti-rabbit IgG (Dako, *www.dako.com*; 1:100 dilution). Bound IgG was visualized with diaminobenzidine. The sections were counterstained with hematoxylin.

RESULTS

Megalin constitutes the major endocytic pathway for clearance of proteins into the proximal tubules and may serve additional yet unrecognized functions in this tissue [22]. To identify changes in renal protein expression caused by inactivation of the receptor gene, the gene expression profiles of kidneys from megalin-deficient and control mice were compared. A total of four individual knockout animals and their respective control littermates were analyzed using the murine oligonucleotide array Mu11k chip B. This chip harbors approximately 6000 murine sequences, including most of the known mouse genes. Total RNA was isolated from renal tissues, labeled and hybridized to the microarrays. The hybridization data were evaluated using the Affymetrix® Gene Expression Analysis Software as described in the **Methods** section.

To obtain information on the overall changes in gene expression the expression data between two individual wild types (Fig. 1A), two knockouts (Fig. 1B) or one wild type and one knockout mouse (Fig. 1C) were compared initially. Using expression scatter analysis, no gross abnormalities in the overall gene expression pattern were identified when wild type and receptor-deficient animals were compared with each other (Fig. 1C). The scattering of the expression levels was similar to the scattering observed between two individual wild type or two receptor-deficient animals, respectively (Fig. 1 A, B).

Next, all genes with significantly altered expression levels in receptor-deficient as compared to control tissue were identified (Table 1). Only changes validated by the Affymetrix® software program as decreased (D) or increased (I) and seen at least in three out of the four experiments were included in this analysis. Application of alternative software programs such as Gene Spring® to evaluate the expression data gave qualitatively identical results (not shown). A total of 19 genes exhibited significant changes in expression pattern, 6 of which were decreased while 13 were increased in knockout mice. Among the genes drastically decreased in receptor-deficient animals was the megalin gene itself, confirming the accuracy of the profiling experiments. Interestingly, most of the genes with altered expression levels could be grouped into a few distinct physiological pathways. These pathways include the cellular vitamin D metabolism, TGF-β1 signal transduction, lipid transport and heavy metal detoxification, suggesting the involvement of megalin in a distinct set of (patho)physiologic processes in the kidney.

Quantitative RT-PCR was employed to confirm the changes in the expression pattern detected by microarray technology. Among others, we analyzed the mRNA levels for CCAAT/enhancer binding protein-β (C/EBP), vitamin D_3-24-hydroxylase (24-HYD) and collagen type IIIα1 (COL3A1) (Fig. 2). The difference in the number of cycles required for each PCR reaction to reach the threshold cycle (ct) value was used to calculate the difference in mRNA levels between wild type and receptor-deficient tissues according to the standard curve method ($2^{\Delta ct}$) . Consistent with the microarray data, the amount of mRNA for 24-HYD was reduced 9.8-fold, whereas mRNAs for C/EBP and COL3A1 were increased 5.5-fold and 5.3-fold in knockout animals, respectively.

24-HYD is a key enzyme in the cellular vitamin D metabolism of proximal tubular cells [23]. These cells take up the precursor 25-OH vitamin D_3 and convert it into two alternative metabolites. They either produce the active hormone 1,25-$(OH)_2$ vitamin D_3 by action of the 25-hydroxyvitamin D_3-1-α-hydroxylase (1α-HYD) or 24,25-$(OH)_2$ vitamin D_3, an inactive derivative, through 24-HYD. The latter pathway is chosen when sufficient 1,25-$(OH)_2$ vitamin D_3 is present in the circulation and the metabolite exerts a negative feedback control on 1α-HYD activity. In contrast, in a state of vitamin D deficiency more 25-(OH) vitamin D_3 in the kidney is converted into 1,25-$(OH)_2$ vitamin D_3 and the activity of the catabolic enzyme 24-HYD is reduced [23].

The decrease in 24-HYD mRNA levels in megalin-deficient kidneys indicated a state of vitamin D deficiency in this animal model. To confirm a concomitant increase in 1α-HYD activity, we analyzed the mRNA

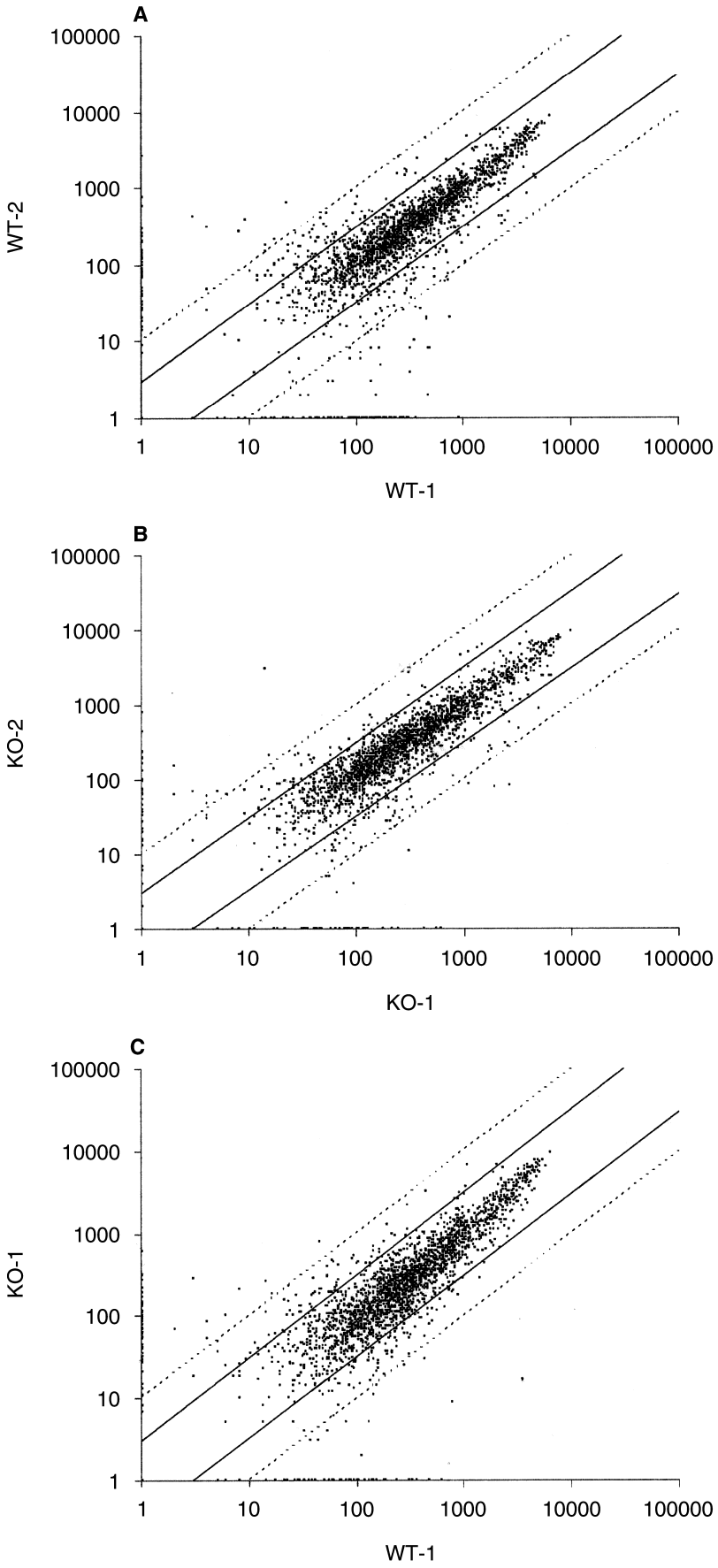

Fig. 1. Expression scatter correlation graphs of wild-type and megalin-deficient mouse kidneys. Genome-wide gene expression levels were compared between two individual wild-types (*A*), two individual knockouts (*B*) or one wild-type and one knockout animal (*C*). Solid lines indicate a difference in expression level by a factor of three; dotted lines denote a difference by a factor of ten. Representative data of one out of four expression profiling experiments are shown.

Table 1. Genes differentially expressed in megalin-deficient as compared to control mouse kidneys

Probe set	Gene function/description	GenBank	Exp. A		Exp. B		Exp. C		Exp. D		N
			Dif	Fold	Dif	Fold	Dif	Fold	Dif	Fold	
Down-regulation in knockouts											
Vitamin D metabolism											
Msa.32856.0_s_at	Megalin	AA109196	D	~−29.9	D	−19	D	~−40.9	D	−12	4/4
Msa.1752.0_s_at	25-hydroxyvitamin D_3 24-hydroxylase	D49438	D	~−12.7	D	~−7.7	D	~−6.2	MD	~−3.7	4/4
Others											
Msa.693.0_f_at	Insulin-like growth factor II (IGF-II)	M36332	NC	−1.3	D	−3.5	MD	−3.4	D	−2.8	3/4
Msa.6321.0_s_at	Non-POU-domain-containing, octamer-binding protein	AA002852	D	−2.4	D	−1.4	D	−1.4	NC	~−1.4	3/4
Msa.2800.0_s_at	Thiazide-sensitive Na-Cl cotransporter	U61085	NC	−1.2	D	−1.7	D	−2	D	−2.3	3/4
Msa.33222.0_f_at	Similar to pyruvate kinase M	AA119868	MD	−1.5	MD	−1.5	NC	−1.9	MD	−1.8	3/4
Up-regulation in knockouts											
TGF-ß pathway											
X52046_s_at	Collagen type III alpha-I (COL3A1)	X52046	I	3.5	I	~9.1	I	~6.0	I	2.5	4/4
Msa.756.0_g_at	HMG-CoA reductase	M62766	I	~3.2	I	3.3	NC	1.6	MI	1.8	3/4
X62940_s_at	TGF-beta stimulated clone-22	X62940	I	1.7	I	2.1	I	1.7	NC	−1.1	3/4
X54149_s_at	MyD118	X54149	I	1.5	I	2.3	I	1.7	NC	1.2	3/4
Lipid transport											
X81627_s_at	Lipocalin-encoding gene 24p3	X81627	I	9.2	I	6.3	NC	1.9	I	2.8	3/4
Msa.2129.0_s_at	SV-40 induced 24p3	W13166	I	~14.7	I	~8.9	I	~5.5	NC	~1.8	3/4
Heavy metal detox.											
Msa.3025.0_s_at	Ceruloplasmin	U49430	MI	3.3	I	2	I	1.7	NC	−1.1	3/4
V00835_f_at	Metallothionein-I	V00835	I	3.1	I	4.3	I	2.9	NC	−6.4	3/4
Others											
Msa.29071.0_s_at	Pol polyprotein	AA087673	I	3.2	I	~18	I	~30.4	I	~23.5	4/4
Msa.30568.0_s_at	Pol polyprotein	AA097626	I	2.6	I	6.8	I	5.9	I	44.3	4/4
Msa.613.0_f_at	Murine leukemia virus modified polytropic provirus	M17327	I	1.8	I	2	I	1.7	NC	1.7	3/4
Msa.19552.0_s_at	Leukemia virus (MuLV) endonuclease	AA013976	I	4.1	I	2.2	NC	1.4	I	~11.1	3/4
X62600_s_at	CCAAT/enhancer binding protein (C/EBP) beta	X62600	MI	2.4	I	9.9	I	5.7	I	3.5	4/4
X70296_s_at	Serine protease inhibitor 4 (Spi4)	X70296	I	3	I	2.1	I	2	NC	1.9	3/4
W10325_s_at	cDNA clone image: 313367 5′	W10325	I	1.9	I	3.8	I	1.5	NC	1.8	3/4

The table depicts all genes that are differentially expressed in 3 (N = 3/4), or 4 out of 4 individual experiments (N = 4/4). Abbreviations are: D, decreased in knockouts; Dif, difference call; fold, fold change; I, increased in knockouts; MD, marginally decreased; MI, marginally increased; NC, not changed. A tilde preceding the fold change value indicates that the expression level for the untreated sample was under the calculated noise level, therefore the fold change is an approximation.

levels of this enzyme. Because the 1α-HYD gene sequence is not present on the Mu11K chip B, RT-PCR was used to quantify the amount of the renal mRNA. Indeed, 1α-HYD mRNA levels were increased fourfold in receptor-deficient kidneys as compared to controls (Fig. 3).

Another group of genes that exhibit increased levels of expression in megalin-deficient kidneys are renal TGF-β1 target genes [24–27]. These include genes for COL3A1, TGF-β1 stimulated clone-22, MyD118 and 3-hydroxy-3-methylglutaryl coenzyme A (HMG-CoA) reductase (Table 1). TGF-β1 is a growth factor that plays a central role in pathophysiological processes in the kidney leading to extracellular matrix deposition. Because signal transduction pathways through TGF-β1 and through 1,25-$(OH)_2$ vitamin D_3 use the same intracellular co-activators, called SMAD proteins, both signaling cascades modulate each other when acting on the same cell. Depending on the cell type, synergistic or antagonistic influences are possible [28]. In renal tissues, 1,25-$(OH)_2$ vitamin D_3 suppresses TGF-β1 activity [29]. To test what mechanism may be responsible for induction of TGF-β1 activity in megalin knockout kidneys we investigated this signaling pathway in more detail. Using in situ hybridization, activation of COL3A1 gene transcription was detected in cells localized in the tubulointerstitial space and around the glomeruli (Fig. 4 A, B). No significant signal was detected in wild type samples (Fig. 4C). Increased transcription in knockout mice resulted in overproduction and extracellular deposition of collagen type

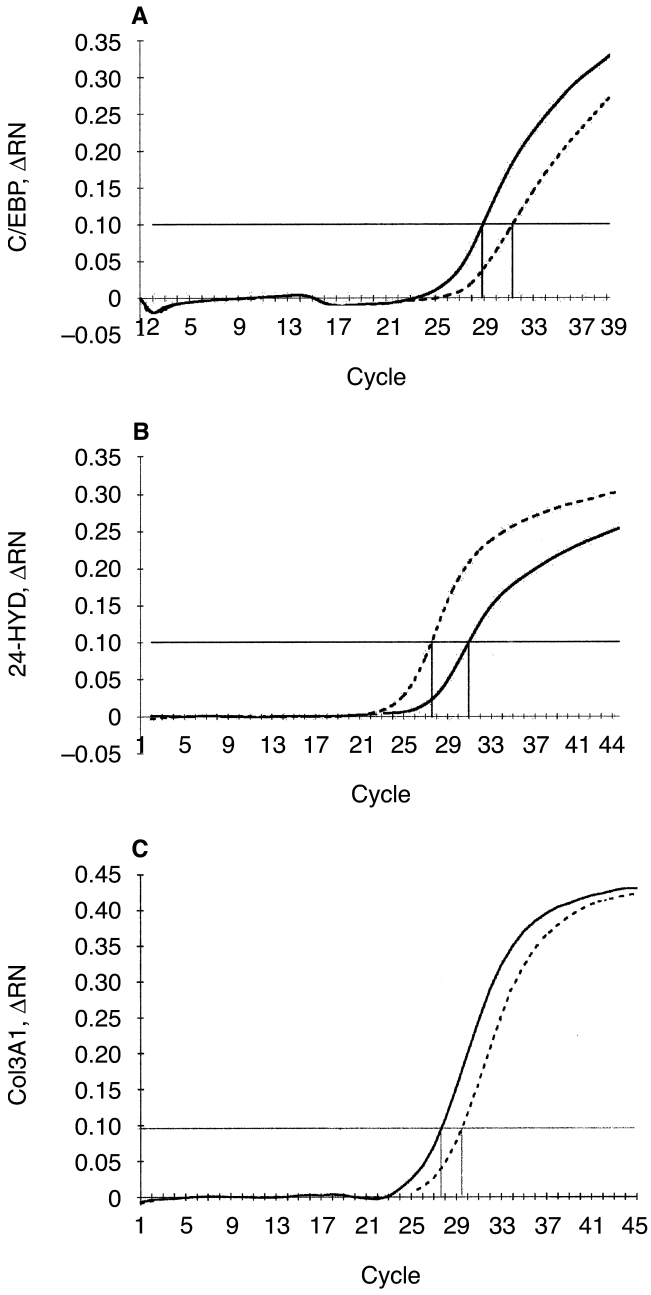

Fig. 2. Quantitative RT-PCR analysis of gene expression in mouse kidneys. Total RNA samples from wild-type (WT) and megalin-deficient mouse kidneys (KO) were analyzed by quantitative RT-PCR to test for expression levels of CCAAT/enhancer binding protein-β (C/EBP), vitamin D-24-hydroxylase (24-HYD) and collagen type IIIα-1 (COL3A1). Symbols are: (thin solid line) CT; (thick solid line) KO; (dashed line) WT. The threshold cycle (ct) value for each reaction is indicated by the horizontal line; ct values for each sample are shown by the vertical lines. The difference in ct values between wild-type and knockout RNA samples was used to calculate the difference in mRNA levels ($2^{\Delta ct}$). Representative data of one out of three experiments are shown.

III α1 protein as was demonstrated by immunohistological inspection of mouse kidney sections (Fig. 5). The overall intensity of collagen type III α1 staining was significantly increased in receptor-deficient tissue (Fig. 5B).

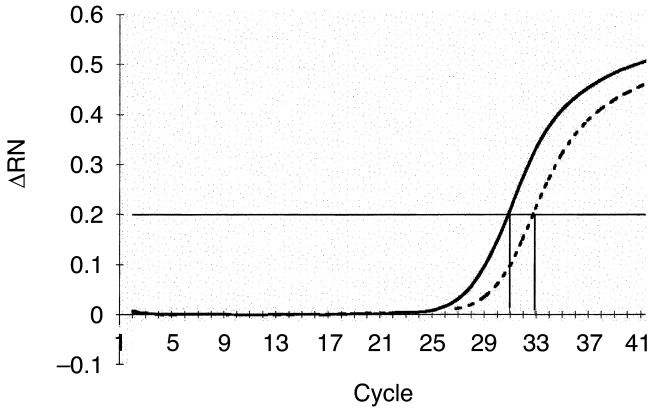

Fig. 3. Quantitative RT-PCR analysis of 25-(OH)-vitamin D_3-1-α-hydroxylase gene expression in mouse kidneys. The levels of 25-(OH)-vitamin D_3-1-α-hydroxylase (1α-HYD) gene expression were evaluated by quantitative RT-PCR in wild-type and megalin knockout mouse kidneys as described in legend to Figure 2. Symbols are: (thin solid line) CT; (thick solid line) KO; (dashed line) WT.

In addition, strong accumulation of the protein was detected in focal areas of the renal cortex, in particular in the perivascular and the interstitial space (Fig. 5 C, D). No such features were observed in wild type kidneys (Fig. 5A), or in tissue incubated with the secondary antibody only (Fig. 5E). The up-regulation of TGF-β1 target genes was not due to an enhanced production of the signaling factor because no increase in renal mRNAs for TGF-β1 or TGF-β2 was seen in megalin-deficient kidneys (Table 2). Furthermore, no significant differences in the total amount of TGF-β1 protein was detected in plasma (10.07 ± 0.6 ng/mL; ± SEM) and kidney (109.9 ± 62.1 pg/mg protein) of knockout animals as compared to controls (plasma, 24.3 ± 17.2 ng/mL; kidney, 111.0 ± 55.0 pg/mg protein). Taken together, these observations suggested an increase in renal TGF-β1 bioactivity in megalin knockout kidneys, possibly as a consequence of reduced vitamin D signaling.

An imbalance in systemic vitamin D homeostasis in receptor-deficient animals was further confirmed when the levels of vitamin D_3 metabolites and parathyroid hormone (PTH) in plasma and urine were analyzed (Table 3). Due to the inability to reabsorb 25-OH vitamin D_3/DBP complexes from the glomerular filtrate, receptor-deficient animals secreted significant amounts of 25-OH vitamin D_3 into the urine. No 25-OH vitamin D_3 was detected in wild-type urine samples. The urinary loss of 25-OH vitamin D_3 resulted in a 68% reduction in the plasma levels of the precursor hormone and, as a consequence, in a 67% decrease in active 1,25-$(OH)_2$ vitamin D_3. The plasma PTH levels were increased significantly indicating secondary hyperparathyroidism as a consequence of hypovitaminosis D.

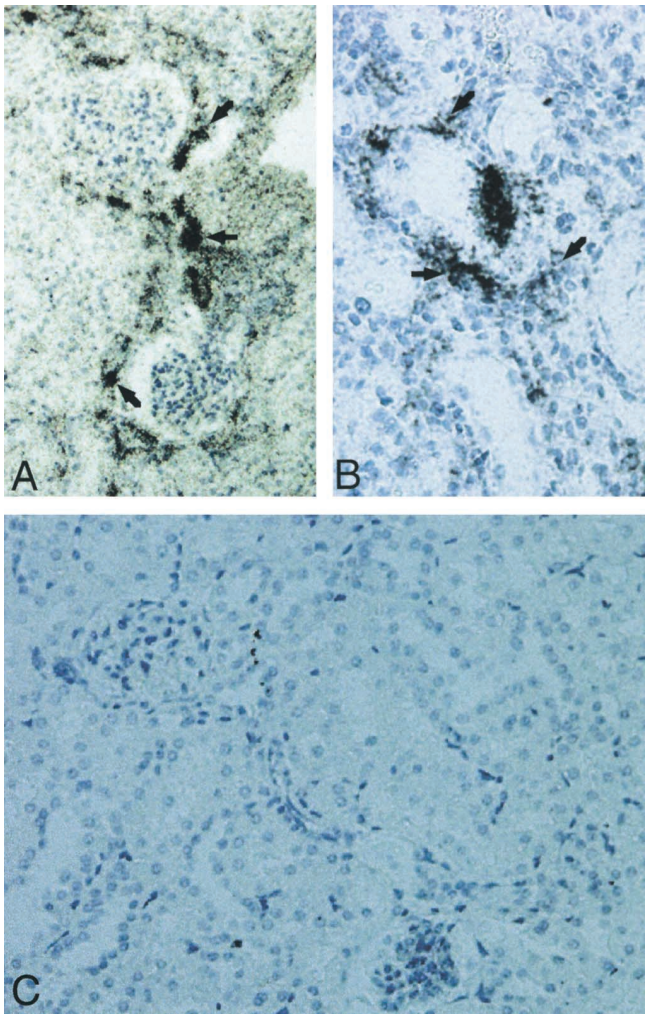

Fig. 4. Localization of collagen type III α-1 gene transcription in megalin-deficient mouse kidneys. Deparaffinized sections from megalin-deficient mouse kidneys were analyzed by in situ hybridization with antisense probes directed against mouse collagen type IIIα-1. Gene overexpression was detected in interstitial cells surrounding the glomeruli (arrows; *A*) and in the peritubular space (arrows; *B*). No signal was seen in wild type control mice (*C*). No signal was obtained with the sense probe (not shown).

DISCUSSION

Previously, megalin-deficient mice have been shown to be unable to take up 25-OH vitamin D_3/DBP complexes from the glomerular filtrate into proximal tubular cells. Inhibition of the receptor in perfused rat kidneys resulted in a significant decrease in the production of 1,25-$(OH)_2$ vitamin D_3. Lack of the receptor coincided with growth retardation and impaired bone calcification in megalin$^{-/-}$ mice [10]. These findings strongly suggest a role for the receptor in renal vitamin D metabolism by delivering 25-OH vitamin D_3 to proximal tubular cells required for production of active 1,25-$(OH)_2$ vitamin D_3. However, many open questions as to the significance of megalin activity in systemic vitamin D metabolism remained to

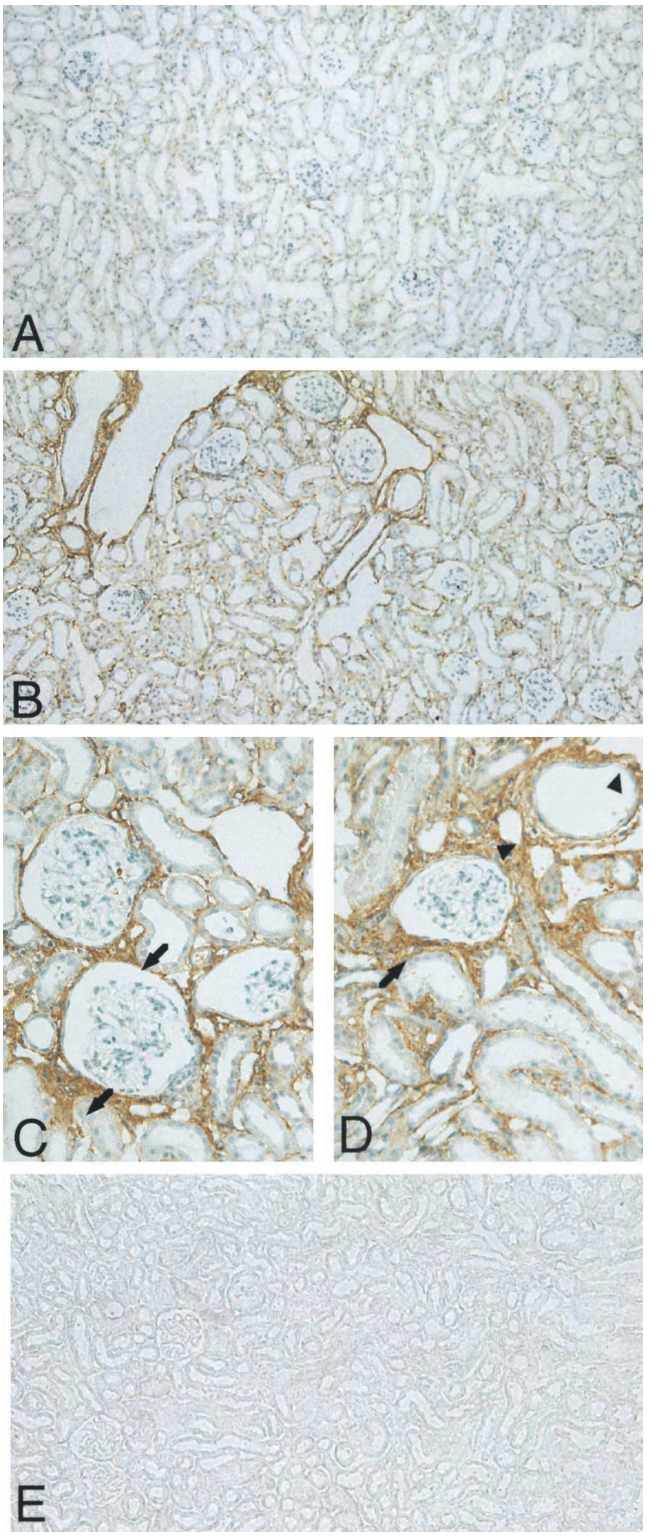

Fig. 5. Immunohistological detection of collagen type III α-1 in wild type and megalin-deficient mouse kidneys. Cryosections of wild type (*A*) and megalin-deficient kidneys (*B*, *C*, *D*) were analyzed for accumulation of collagen type III α-1 using immunohistology. Deposition of the protein was detected in perivascular (arrowhead) and interstitial regions (arrow) of receptor-deficient (B–D) but not in control tissue (A). No signal was seen with application of the secondary peroxidase-conjugated antibody only (*E*).

Table 2. Expression levels of TGF-β1 and TGF-β2 in megalin-deficient as compared to control mouse kidneys

Probe set	Gene description	Exp. A		Exp.B		Exp. C		Exp. D	
		Dif	Fold	Dif	Fold	Dif	Fold	Dif	Fold
Msa.1226.0_s_at	TGF-β1 gene 5′ end and promoter region	NC	~1.2	NC	−1.1	NC	~−1.1	NC	−1.2
Msa.9718.0_s_at	TGF-β1 precursor	NC	~−1.5	NC	~−1.2	NC	~−1.9	NC	~−2.1
X57413_s_at	TGF-β2 cDNA	NC	−1.2	NC	−1.2	NC	−1.1	NC	−1.3

NC, not changed.

Table 3. Endocrine parameters in wild type and megalin-deficient mice

Parameters	Genotypes				
	+/+	*N*	−/−	*N*	*P*
Plasma					
25-(OH) D_3 *nmol/L*	86.6 ± 20.4	5	27.5 ± 8.3	4	<0.01
1,25-$(OH)_2$ D_3 *pmol/L*	130.0 ± 42.3	5	43.3 ± 17.5	4	<0.01
PTH 1-38 *pmol/L*	49.8 ± 4.4	8	68.5 ± 1.8	3	<0.02
Urine					
25-(OH) D_3 *nmol/mmol creatinine*	ND	5	2.51 ± 0.29	4	<0.01[a]
PTH 1-38 *pmol/L*	87.5 ± 29	8	374.0 ± 48	4	<0.002

Values are given as mean (± standard error of the mean). The statistical significance of the values (*P*) was determined by the Student *t* or Mann-Whitney test ([a]). *N*, number of animals; ND, not detectable.

be addressed. For example, no data on plasma 1,25-$(OH)_2$ vitamin D_3 and PTH levels were available due to the small number of surviving knockouts and the inability to obtain enough plasma samples for measurement. Also, it remained unclear to what extend the urinary loss of 25-OH vitamin D_3 in the knockout mice really impaired renal and systemic vitamin D homeostasis. Continued breeding efforts to obtain more surviving megalin$^{-/-}$ animals and novel technological advances in molecular phenotyping of animal models, now enabled us to investigate the consequence of urinary loss of 25-OH vitamin D_3/DBP complexes in the megalin knockout mouse model in more detail. Data generated by expression profiling, immunohistology and endocrine analysis provide further strong evidence for a crucial role of megalin in renal vitamin D_3 homeostasis. Our results demonstrate (*a*) a significant decrease in plasma levels of 25-OH vitamin D_3 and 1,25-$(OH)_2$ vitamin D_3 in megalin knockout mice, (*b*) a compensatory transcriptional regulation of enzymes in the cellular vitamin D metabolism and of renal TGF-β1 target genes, and (*c*) an increase in plasma PTH levels, indicative of secondary hyperparathyroidism as a consequence of plasma vitamin D deficiency.

The kidney constitutes one of the prime tissues involved in the regulation of the systemic calcium and bone metabolism. Therefore, it represents an appropriate target to uncover potential abnormalities in calcium homeostasis as a consequence of megalin deficiency. Transcriptional up-regulation of 1α-HYD indicates a status of plasma vitamin D deficiency and a lack of sufficient quantities of 1,25-$(OH)_2$ vitamin D_3 in this mouse model (Fig. 3). This conclusion is confirmed by a concomitant decrease in renal 24-HYD expression (Fig. 2).

Further support for a role of megalin in renal vitamin D metabolism stems from the induction of renal TGF-β1 target genes in knockout mice. Different pathways result in activation of TGF-β1 and downstream genes in the kidney. The most common mechanism involves pathophysiologic processes leading to tubulointerstitial fibrosis (TIF), a progressive degeneration characterized by extracellular matrix accumulation. TIF is commonly observed in cases of severe renal dysfunction such as obstructive nephropathy or glomerular sclerosis [30–32]. Hallmarks of the disease are the infiltration of activated monocytes into the interstitial space. There, these cells release TGF-β1 that induces transcriptional activation of downstream targets such as genes for laminin and collagens. Most likely, this mechanism is not responsible for the induction of TGF-β1 pathways in kidneys lacking megalin. Pathological processes leading to up-regulation of TGF-β1 expression are characterized by dramatic histological irregularities of renal tissues including thickening of the basement membranes, degeneration of proximal tubular structures and glomerular lesions [30–32]. Such changes do not occur in receptor-deficient kidneys as shown here (Fig. 5) and in earlier studies [9, 10]. Furthermore, no increases in TGF-β1 mRNA or protein levels were detected in knockout mice (Table 2). Rather, novel findings on the interaction of signaling cascades through TGF-β1 and 1,25-$(OH)_2$ vitamin D_3 suggest a more obvious reason for up-regulation of TGF-β1 pathways in megalin$^{-/-}$ mice. TGF-β1 regulates target gene transcription through activation of SMAD proteins, which

act as intracellular co-activators and transcription factors. SMAD 3, one component of this pathway also acts as a cofactor to the vitamin D receptor [28]. Thus, TGF-β1 and vitamin D signaling pathways converge on the same intracellular activator and mutually affect each other when active on the same cell type. In the kidney, increased signaling through 1,25-$(OH)_2$ vitamin D_3 was shown to reduce the activity of TGF-β1 without affecting expression of the protein [29]. In the converse situation, low vitamin D levels, as in megalin knockout mice, can be expected to increase TGF-β1 bioactivity.

Of the four TGF-β1 target genes induced in megalin-deficient kidneys, the physiological roles for COL3A1 and HMG-CoA reductase in TGF-β1 induced fibrotic processes is well established [24, 25]. The significance of the two other genes, the TGF-β1 stimulated clone-22 and MyD118, is less evident. Both genes have been identified as TGF-β1 targets in salivary gland tumor (clone 22) [26] and myeloid leukemia cell lines (MyD118) [27]; their functions remain unknown. Regardless of their exact physiological roles, induction of transcription proves the up-regulation of the TGF-β1 signaling pathway in megalin-deficient kidneys.

Finally, support for an important role of megalin in renal vitamin D and calcium homeostasis comes from the analysis of parathyroid hormone (PTH) levels in urine and plasma of the knockout mice. Increased plasma and urine levels of PTH indicate a status of secondary hyperparathyroidism as a consequence of vitamin D deficiency (Table 3). Interestingly, the excretion of PTH 1-38 is increased fourfold in the urine of megalin$^{-/-}$ animals. This increase is higher than the actual increase in PTH 1-38 levels in the circulation (1.5-fold; Table 3). This finding confirms an earlier observation on the role of megalin in PTH action [33]. PTH 1-38 is considered the active fragment of the hormone that is produced in the parathyroid in a state of hypocalcemia. It acts on its cognate PTH receptor expressed in proximal tubular cells of the kidney, inducing 1α-HYD activity and 1,25-$(OH)_2$ vitamin D_3 production. Our earlier study demonstrated that megalin is co-expressed with the PTH receptor on the apical surface of proximal tubular cells and that it counter-regulates this receptor by clearing PTH 1-38 fragments from the glomerular filtrate [33]. Thus, the increase in PTH 1-38 levels in the urine of megalin-deficient mice likely represents the combined effects of an increased PTH production in the parathyroid and a decreased tubular clearance.

In conclusion, genome-wide expression profiling has highlighted important functions played by the endocytic receptor megalin in the proximal tubules of the kidney. Involvement of this receptor in vitamin D homeostasis has already been suggested previously [10, 33]. Data on the altered gene expression in megalin$^{-/-}$ kidneys now provide additional evidence to support a role of this receptor in renal vitamin D metabolism and systemic calcium homeostasis by mediating tubular uptake of the precursor 25-OH vitamin D_3 and by clearing PTH 1-38. Additional yet unrecognized functions of the receptor may be uncovered by further investigation of other groups of genes differentially expressed in this mouse model including lipid transport through the lipocalin 24p3 or heavy metal detoxification.

ACKNOWLEDGMENTS

Studies presented here were funded in part by grants from the Deutsche Forschungsgemeinschaft, the Max-Delbrueck-Center for Molecular Medicine, the Karin Elise Jensen Foundation and the University of Aarhus. We are indebted to C. Räder, H. Schulz, A. Morell and J. Czychi for expert technical assistance, to F.P. Armbruster (Immundiagnostik Bensheim) for PTH 1-38 measurements, and to N. Hübner for helpful discussions.

Reprint requests to Dr. Thomas E. Willnow, Max-Delbrueck-Center for Molecular Medicine, Robert-Roessle-Strasse 10, D-13125 Berlin, Germany.
E-mail: willnow@mdc-berlin.de

REFERENCES

1. Zheng G, Bachinsky DR, Stamenkovic I, *et al*: Organ distribution in rats of two members of the low-density lipoprotein receptor gene family, gp330 and LRP/a_2MR, and the receptor-associated protein (RAP). *J Histochem Cytochem* 42:531–542, 1994
2. Christensen EI, Nielsen S, Moestrup SK, *et al*: Segmental distribution of the endocytosis receptor gp330 in renal proximal tubules. *EJCB* 66:349–364, 1995
3. Farquhar MG, Kerjaschki D, Lundstrom M, *et al*: gp330 and RAP: The Heymann nephritis antigenic complex. *Ann N Y AcadSci* 737:96–113, 1994
4. Raychowdhury R, Niles JL, McCluskey RT, *et al*: Autoimmune target in Heymann nephritis is a glycoprotein with homology to the LDL receptor. *Science* 244:1163–1165, 1989
5. Saito A, Pietromonaco S, Loo AK-C, *et al*: Complete cloning and sequencing of rat gp330/"megalin." A distinctive member of the low density lipoprotein receptor gene family. *Proc Natl Acad Sci USA* 91:9725–9729, 1994
6. Hjalm G, Murray E, Crumley G, *et al*: Cloning and sequencing of human gp330, a Ca(2+)-binding receptor with potential intracellular signaling properties. *Eur J Biochem* 239:132–137, 1996
7. Moestrup SK, Cui S, Vorum H, *et al*: Evidence that epithelial glycoprotein 330/ megalin mediates uptake of polybasic drugs. *J Clin Invest* 96:1404–1413, 1995
8. Orlando RA, Rader K, Authier F, *et al*: Megalin is an endocytic receptor for insulin. *J Am Soc Nephrol* 9:1759–1766, 1998
9. Leheste JR, Rolinski B, Vorum H, *et al*: Megalin knockout mice as an animal model of low molecular weight proteinuria. *Am J Pathol* 155:1361–1370, 1999
10. Nykjaer A, Dragun D, Walther D, *et al*: An endocytic pathway essential for renal uptake and activation of the steroid 25-(OH) vitamin D_3. *Cell* 96:507–515, 1999
11. Moestrup SK, Kozyraki R, Kristiansen M, *et al*: The intrinsic factor-vitamin B12 receptor and target of teratogenic antibodies is a megalin-binding peripheral membrane protein with homology to developmental proteins. *J Biol Chem* 273:5235–5242, 1998
12. Birn H, Fyfe J, Jacobsen C, *et al*: Cubilin is an albumin binding protein important for renal albumin reabsorption. *J Clin Invest* 105:1353–1361, 2000
13. Biemesderfer D, Nagy T, DeGray B, *et al*: Specific association of megalin and the Na^+/H^+ exchanger isoform NHE3 in the proximal tubule. *J Biol Chem* 274:17518–17524, 1999
14. Burmeister R, Boe IM, Nykjaer A, *et al*: A two-receptor pathway for catabolism of Clara cell secretory protein in the kidney. *J Biol Chem* 276:13295–13301, 2001

15. Gotthardt M, Trommsdorff M, Nevitt MF, *et al*: Interactions of the low density lipoprotein receptor gene family with cytosolic adaptor and scaffold proteins suggest diverse biological functions in cellular communication and signal transduction. *J Biol Chem* 275:25616–25624, 2000
16. Rader K, Orlando RA, Lou X, *et al*: Characterization of ANKRA, a novel ankyrin repeat protein that interacts with the cytoplasmic domain of megalin. *J Am Soc Nephrol* 11:2167–2178, 2000
17. Oleinikov AV, Zhao J, Makker SP: Cytosolic adaptor protein Dab2 is an intracellular ligand of endocytic receptor gp600/megalin. *Biochem J* 347(Pt 3):613–621, 2000
18. Patrie KM, Drescher AJ, Goyal M, *et al*: The membrane-associated guanylate kinase protein MAGI-1 binds megalin and is present in glomerular podocytes. *J Am Soc Nephrol* 12:667–677, 2001
19. Willnow TE, Hilpert J, Armstrong SA, *et al*: Defective forebrain development in mice lacking gp330/megalin. *Proc Natl Acad Sci USA* 93:8460–8464, 1996
20. Harkin DP: Uncovering functionally relevant signaling pathways using microarray-based expression profiling. *Oncologist* 5:501–507, 2000
21. Zhu H, Cong JP, Mamtora G, *et al*: Cellular gene expression altered by human cytomegalovirus: Global monitoring with oligonucleotide arrays. *Proc Natl Acad USA* 95:14470–14475, 1998
22. Christensen EI, Birn H, Verroust P, *et al*: Membrane receptors for endocytosis in the renal proximal tubules. *Inter Rev Cytol* 180: 237–284, 1998
23. Henry HL, Norman AW: Vitamin D: Metabolism and biological actions. *Ann Rev Nutr* 4:493–520, 1984
24. Kim SI, Kim HJ, Han DC, *et al*: Effect of lovastatin on small GTP binding proteins and on TGF-beta1 and fibronectin expression. *Kidney Int* 58(Suppl 77):S88–S92, 2000
25. Eberlein M, Heusinger-Ribeiro J, Goppelt-Struebe M: Rho-dependent inhibition of the induction of connective tissue growth factor (CTGF) by HMG CoA reductase inhibitors (statins). *Br J Pharmacol* 133:1172–1180, 2001
26. Hino S, Kawamata H, Uchida D, *et al*: Nuclear translocation of TSC-22 (TGF-beta-stimulated clone-22) concomitant with apoptosis: TSC-22 as a putative transcriptional regulator. *Biochem Biophys Res Commun* 278:659–664, 2000
27. Selvakumaran M, Lin HK, Sjin RT, *et al*: The novel primary response gene MyD118 and the proto-oncogenes myb, myc, and bcl-2 modulate transforming growth factor beta 1-induced apoptosis of myeloid leukemia cells. *Mol Cell Biol* 14:2352–2360, 1994
28. Yanagisawa J, Yanagi Y, Masuhiro Y, *et al*: Convergence of transforming growth factor-β and vitamin D signaling pathways on SMAD transcriptional co-activators. *Science* 283:1317–1321, 1999
29. Aschenbrenner JK, Sollinger HW, Becker BN, *et al*: 1,25-(OH_2) D_3 alters transforming growth factor-β signaling pathway in renal tissues. *J Surg Res* 100:171–175, 2001
30. Isaka Y, Tsujie M, Ando Y, *et al*: Transforming growth factor-beta 1 antisense oligodeoxynucleotides block interstitial fibrosis in unilateral ureteral obstruction. *Kidney Int* 58:1885–1892, 2000
31. Adhikary LP, Yamamoto T, Isome M, *et al*: Expression profile of extracellular matrix and its regulatory proteins during the process of interstitial fibrosis after anti-glomerular basement membrane antibody-induced glomerular sclerosis in Sprague-Dawley rats. *Pathol Int* 49:716–725, 1999
32. Taal MW, Zandi-Nejad K, Weening B, *et al*: Proinflammatory gene expression and macrophage recruitment in the rat remnant kidney. *Kidney Int* 58:1664–1676, 2000
33. Hilpert J, Nykjaer A, Jacobsen C, *et al*: Megalin antagonizes activation of the parathyroid hormone receptor. *J Biol Chem* 274: 5620–5625, 1999